cmgh
CELLULAR AND MOLECULAR
GASTROENTEROLOGY AND HEPATOLOGY

ORIGINAL RESEARCH

Formation of Human Colonic Crypt Array by Application of Chemical Gradients Across a Shaped Epithelial Monolayer

Yuli Wang,[1] Raehyun Kim,[2] Dulan B. Gunasekara,[1] Mark I. Reed,[1] Matthew DiSalvo,[2] Daniel L. Nguyen,[1] Scott J. Bultman,[3] Christopher E. Sims,[1] Scott T. Magness,[2] and Nancy L. Allbritton[1,2]

[1]Department of Chemistry, [3]Department of Genetics, University of North Carolina, Chapel Hill, North Carolina; [2]Joint Department of Biomedical Engineering, University of North Carolina, Chapel Hill, and North Carolina State University, Raleigh, North Carolina

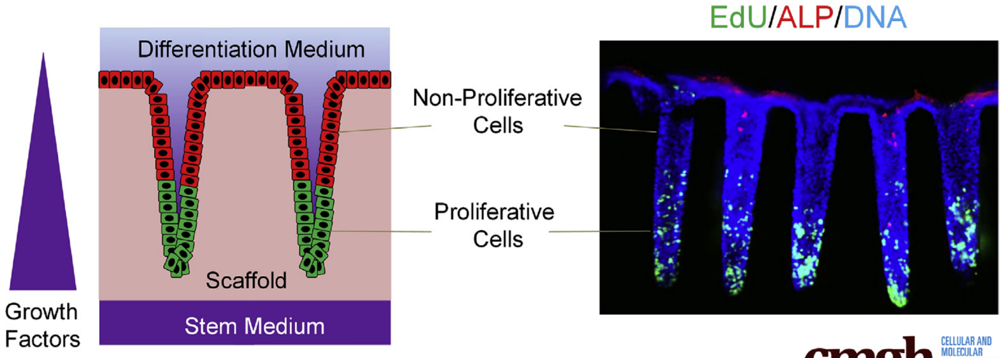

SUMMARY

Human colonic epithelia were cultured on a microfabricated scaffold under a growth factor gradient to generate crypt structures. Responses to cytokines or bacterial metabolite gradients were assessed from altered stem and differentiated cell numbers and locations.

BACKGROUND & AIMS: The successful culture of intestinal organoids has greatly enhanced our understanding of intestinal stem cell physiology and enabled the generation of novel intestinal disease models. Although of tremendous value, intestinal organoid culture systems have not yet fully recapitulated the anatomy or physiology of the in vivo intestinal epithelium. The aim of this work was to re-create an intestinal epithelium with a high density of polarized crypts that respond in a physiologic manner to addition of growth factors, metabolites, or cytokines to the basal or luminal tissue surface as occurs in vivo.

METHODS: A self-renewing monolayer of human intestinal epithelium was cultured on a collagen scaffold microfabricated with an array of crypt-like invaginations. Placement of chemical factors in either the fluid reservoir below or above the cell-covered scaffolding created a gradient of that chemical across the growing epithelial tissue possessing the in vitro crypt structures. Crypt polarization (size of the stem/proliferative and differentiated cell zones) was assessed in response to gradients of growth factors, cytokines, and bacterial metabolites.

RESULTS: Chemical gradients applied to the shaped human epithelium re-created the stem/proliferative and differentiated cell zones of the in vivo intestine. Short-chain fatty acids applied as a gradient from the luminal side confirmed long-standing hypotheses that butyrate diminished stem/progenitor cell proliferation and promoted differentiation into absorptive colonocytes. A gradient of interferon-γ and tumor necrosis factor-α significantly suppressed the stem/progenitor cell proliferation, altering crypt formation.

CONCLUSIONS: The in vitro human colon crypt array accurately mimicked the architecture, luminal accessibility, tissue polarity, cell migration, and cellular responses of in vivo intestinal crypts. *(Cell Mol Gastroenterol Hepatol 2018;5:113–130; https://doi.org/10.1016/j.jcmgh.2017.10.007)*

Keywords: Intestinal Epithelial Cells; Intestine-On-A-Chip; Stem Cell Niche; Polarized Crypt.

See editorial on page 161.

Organ-on-chip technology is a rapidly advancing field that is expected to usher in completely new approaches to drug testing and biological study.[1] Organ-on-chip devices strive to combine microengineered environments with living cells to produce physiologic systems. Devices are being developed to recapitulate the structure and function of a variety of organs, including liver, heart, and lung.[2] The expectation is that these devices, particularly when incorporating human cells, will create a revolution in the study of human biology and drug development.[3,4] Among these systems, the large intestine especially represents an important organ for in vitro study of intestinal physiology and the evaluation of the effects of pharmaceutical agents and microbial metabolites. For example, pharma and food companies are intensely interested in screening the gut microbiome and the effects of prebiotics and probiotics by virtue of their roles in metabolism and their influences on the human body.[5,6] Despite this importance, major challenges exist in creating an in vitro intestinal epithelium because the intestinal lining is a highly polarized tissue and primary gut epithelium rapidly dies in standard culture. Current gold standard methods for intestinal assays use tumor cell lines, such as Caco-2, and animals.[7–10] This is problematic because tumor cells lack many of the features of normal intestinal tissue and animal models are expensive and increasingly fraught by ethical concerns.

Recently developed intestinal stem-cell culture methods are expected to dramatically improve this situation.[11,12] It now is possible to create multicellular structures known as organoids or mini-guts from primary animal and human stem cells.[13–15] These structures possess self-renewing stem cells and their differentiated progeny to reproduce intestinal epithelium in a culture dish. The potential for the organoid technology is enormous; nevertheless, the enclosed cystic, spherical architecture of organoids presents severe limitations.[16–20] Because of the bulk properties of the matrix and lack of spatial control of growth factors (eg, biochemical gradients), intestinal organoids form embedded within a paddy of Matrigel (Corning, Tewksbury, MA) with an enclosed, inaccessible lumen and random buds lacking distinct stem/transit-amplifying and differentiated cell compartments.[21,22] These characteristics preclude the use of the organoid system in numerous applications and a true living construct suitable for assay of dietary metabolites, cytokines, microorganisms, and drug interactions has not been available.[23,24] What is needed is the ability to recreate the epithelium of the organoid system in an open-faced geometry while maintaining its cellular composition, polarity, and physiology. Our group has been striving to achieve such an intestine-on-chip system for both small and large intestines.[25–32]

To address the limitation of the enclosed lumen of organoids, we surveyed a variety of biomaterials, and identified a collagen hydrogel scaffold that enabled a self-renewing planar monolayer culture of colonic epithelial cells with properties similar to those of organoids, but whose luminal surface was readily accessible.[25] Nevertheless, these monolayers lacked the 3-dimensional architecture and tissue polarity of in vivo colon crypts. To overcome this shortcoming, in the current study we incorporated microfabrication of the hydrogel scaffold and spatial control of growth factors in a simple-to-use open format. Primary cells from a colonoscopic biopsy were first expanded in the aforementioned monolayer system. The collagen hydrogel scaffold was microfabricated in a microwell architecture possessing the shape of human colonic crypts. A gradient of growth factors along the crypts' z-axis was used to induce the polarization of the crypts such that stem/progenitor cells were confined to the basal region, while nonproliferative cells were situated along the upper and luminal aspects of the crypts. The in vitro human colonic crypts were compared with native in vivo colon crypts in terms of architecture, luminal patency, tissue polarity, and cell migration. To show the utility of this organ-on-a-chip system, the platform was used to study the impact of metabolites and cytokines on cellular proliferation and location within the tissue.

Materials and Methods

Cell Culture Media

The media compositions are listed in Tables 1 and 2. The culture media (expansion medium [EM], stem medium [SM], and differentiation medium [DM]) for human colonic crypts and epithelial cells were prepared from a mixture of advanced Dulbecco's modified Eagle medium/F12 medium (12634010; ThermoFisher, Waltham, MA) and Wnt-3A, R-spondin 3, noggin (WRN) conditioned medium (see later) at a volumetric ratio of 1:1, and supplemented with 1× GlutaMAX (35050061; ThermoFisher), 1× B27 supplement (12587010; ThermoFisher), 10 mmol/L HEPES (15630-080; ThermoFisher), 1.25 mmol/L N-acetyl cysteine (194603; MP Bio, Santa Ana, CA), 10 mmol/L nicotinamide (N0636; Sigma-Aldrich, St. Louis, MO), 50 ng/mL epidermal growth factor (315-09; Peprotech, Rocky Hill, NJ), 10 nmol/L gastrin (AS-64149; Anaspec, Fremont, CA), 10 nmol/L prostaglandin E2 (14010; Cayman Chemicals, Ann Arbor, MI), 3 μmol/L SB202190 (S1077; Selleckchem, Houston, TX), 100 U/mL penicillin-streptomycin (15140122; ThermoFisher), and 50 μg/mL primocin (ant-pm-1; InvivoGen, San Diego, CA).[33] A total of 10 μmol/L Y27632 (A3008-200; ApexBio, Houston, TX) was used in the first 48 hours after cell plating to prevent dissociation-induced cell apoptosis. WRN

Abbreviations used in this paper: **ALP, alkaline phosphatase; BSA, bovine serum albumin; DM, differentiation medium; DM-B, differentiation medium plus 5 mmol/L butyrate; DM-D, DM plus 10 μmol/L DAPT; EDC, 1-ethyl-3-(3-dimethylaminopropyl)carbodiimide hydrochloride; EdU, 5-ethynyl-20-deoxyuridine; ELISA, enzyme-linked immunosorbent assay; EM, expansion medium; IFN-γ, interferon-γ; KRT20, cytokeratin 20; Muc2, mucin 2; NHS, N-hydroxysuccinimide; Olfm4, olfactomedin-4; P, passage; PBS, phosphate-buffered saline; PDMS, polydimethylsiloxane; PTFE, polytetrafluoroethylene; SCFA, short-chain fatty acid; SEM, scanning electron microscope; SM, stem medium; TNF-α, tumor necrosis factor-α; ZO-1, zonula occludens-1.**

Most current article

© 2018 The Authors. Published by Elsevier Inc. on behalf of the AGA Institute. This is an open access article under the CC BY-NC-ND license (http://creativecommons.org/licenses/by-nc-nd/4.0/).

2352-345X
https://doi.org/10.1016/j.jcmgh.2017.10.007

Table 1. Supplier, Catalog Number, Stock Solution Concentration, and Storage Condition of Reagents

Reagent	Suppliers	Catalog number	Stock solution	Storage
WRN–conditioned medium	Made in-house			-20°C
Advanced DMEM/F12	ThermoFisher	12634-010		4°C
GlutaMax	ThermoFisher	35050061	100×	4°C
HEPES	ThermoFisher	15630-080	1 mol/L	4°C
Gentamycin	ThermoFisher	15750060	50 mg/mL	4°C
Primocin	InvivoGen	ant-pm-1	50 mg/mL	-20°C
B27	ThermoFisher	12587010	50×	-20°C
N-acetyl cysteine	MP Bio	194603	1 mol/L in PBS	-20°C
Murine EGF	Peprotech	315-09	250 μg/mL in 0.1% BSA	-20°C
Nicotinamide	Sigma	N0636-100G	1 mol/L in PBS	-20°C
Gastrin	Anaspec	AS-64149	1 mg/mL in 0.1% BSA	-20°C
Prostaglandin E2	Cayman Chemicals	14010	1 mmol/L in DMSO	-20°C
A83-01	Sigma	SML0788	5 mmol/L in DMSO	-20°C
SB202190	Selleckchem	S1077	30 mmol/L in DMSO	-20°C
Y27632	ApexBio	A3008-200	10 mmol/L in PBS	-20°C
Sodium butyrate	Acros Organics	263190050	500 mmol/L in PBS	-20°C
DAPT	Xcessbio	M60023-5	10 mmol/L in DMSO	-20°C
TNF-α	Peprotech	300-01A	10 μg/mL in 0.1% BSA	-20°C
IFN-γ	Peprotech	300-02	10 μg/mL in 0.1% BSA	-20°C

DMEM, Dulbecco's modified Eagle medium; DMSO, dimethyl sulfoxide; EGF, epidermal growth factor.

conditioned medium was prepared from L-WRN cells (CRL-3276; ATCC, Manassas, VA) following a published protocol.[14] This cell line produces Wnt-3A, R-spondin 3, and noggin. EM was used to expand the epithelial cell numbers as monolayers or organoids. A83-01 (SML0788; Sigma), a transforming growth factor-β inhibitor, was not included in the EM. SM and DM both contained A83-01 (500 ng/mL) because the cells adopted a more columnar morphology under these conditions.

Table 2. Formulation of Culture Media for Human Colonic Epithelial Cells

Reagent	EM	SM	DM
WRN–conditioned medium	50 vol%	50 vol%	
Advanced DMEM/F12	50 vol%	50 vol%	100 vol%
GlutaMax	1×	1×	1×
HEPES	10 mmol/L	10 mmol/L	10 mmol/L
Primocin	50 μg/mL	50 μg/mL	50 μg/mL
N-acetyl cysteine	1.25 mmol/L	1.25 mmol/L	1.25 mmol/L
Murine EGF	50 ng/mL	50 ng/mL	50 ng/mL
Nicotinamide	10 mmol/L		
B27	1×		
Gastrin	10 nmol/L		
PGE2	10 nmol/L		
A83-01		500 nmol/L	500 nmol/L
SB202190	3 μmol/L		
Y27632	10 μmol/L[a]		

DMEM, Dulbecco's modified Eagle medium; EGF, epidermal growth factor.

[a] Used in the first 48 hours after cell plating to prevent dissociation-induced cell apoptosis.

Isolation of Crypts From Human Colonic Biopsy Specimens

Biopsy specimens of human colonic epithelium were obtained during routine screening colonoscopies performed at University of North Carolina's Hospital Meadowmont Endoscopy Center with consent of the patient (under the approved University of North Carolina Institutional Review Board #14-2013). Crypts were isolated from the biopsy specimens by incubation with EDTA (2 mmol/L) and dithiothreitol (0.5 mmol/L) in an isolation buffer for 75 minutes at 20°C followed by vigorous shaking in a 15-mL conical tube. The isolation buffer was composed of 5.6 mmol/L Na_2HPO_4, 8.0 mmol/L KH_2PO_4, 96.2 mmol/L NaCl, 1.6 mmol/L KCl, 43.4 mmol/L sucrose, and 54.9 mmol/L D-sorbitol, pH = 7.4.[13] Hundreds of crypts were released from each biopsy, and the crypts were placed into either monolayer or organoid culture within 30 minutes of isolation.

Organoid Culture With Matrigel Embedding

Released crypts were embedded in Matrigel for organoid culture as described previously.[13,14] Briefly, 500 crypts were suspended in 100 μL of cold Matrigel (356235; Corning, Tewksbury, MA) and then 20 μL of this suspension was added to each well of a 24-well plate. After Matrigel gelation at 37°C for 15 minutes, 500 μL of EM was added to each well. The medium was changed every 48 hours. Y27632 was added to the medium only for the first 48 hours. Every 5 to 7 days the organoids were dissociated with Accutase (07920; Stemcell

Technologies, Cambridge, MA) and cultured on a new 24-well plate after dilution of the cells by one third.

Monolayer Culture on a Neutralized Collagen Hydrogel

Human colonic epithelial cells were expanded as a monolayer on a neutralized collagen hydrogel as described previously.[25] To prepare 36 mL of a neutralized collagen solution (1 mg/mL), 7.4 mL of collagen (356236; Corning; rat tail, type I, 4.89 mg/mL in 20 mmol/L acetic acid) was mixed with 170 μL of sodium hydroxide (stock concentration of 1 N, working concentration of 23 mmol/L), 720 μL of HEPES (15630080; ThermoFisher; stock concentration of 1 mol/L, working concentration of 20 mmol/L), 2.16 mL of sodium bicarbonate (25-035-CI; Corning; stock concentration of 7.5% wt/vol, working concentration of 0.45% wt/vol), 3.6 mL of 10× phosphate-buffered saline (PBS) (46-013-CM; Corning; working concentration of 1×), and 21.95 mL of deionized water on ice. The mixture was added to 6-well plates (T1006; Denville, Holliston, MA) at 1 mL per well. The plates were incubated at 37°C for 1 hour to generate a clear hydrogel. Four milliliters of PBS was added to each well to hydrate the hydrogel. The plates were placed in a sealed plastic bag and stored at room temperature for up to 3 months. The hydrogel was incubated in PBS buffer for at least 15 days before cell culture. This incubation step was critical for successful culture of the self-renewing epithelial cells and may result in a change in stiffness and other hydrogel properties as the gel matured over the 15-day time span.

Before plating crypts or epithelial cells, the collagen hydrogels were rinsed 3 times with 4 mL of PBS for 5 minutes to remove accumulated salt as a result of water evaporation during storage. Isolated crypts were placed on the top of the collagen hydrogel at a density of 500 crypts/well of a 6-well plate and overlaid with EM (4 mL). The medium was changed every 48 hours. When the cell coverage was greater than 80% (typically 5–7 days), the monolayers were passaged by a gentle 2-step dissociation method.[25] The first step was to detach the monolayer from the collagen hydrogel by breaking the hydrogel into pieces by repeated pipetting followed by incubating the hydrogel with 500 U/mL collagenase at 37°C for 10 minutes. The second step was to further split the cell fragments into smaller pieces by incubating the mixture with 150 μL of EDTA (0.5 mmol/L) and Y27632 (10 μmol/L) in PBS at 37°C for 5 minutes. The monolayers again were dispersed by pipetting up and down 30 times using a 200-μL pipet tip. The cell fragments were resuspended in medium and subcultured on a new collagen hydrogel at a passage ratio of 1:3. To ensure that the cells possessed normal chromosomes, cells were karyotyped (KaryoLogic, Inc, Research Triangle Park, NC) at passage (P)7 and P11. Twenty cells from each sample were analyzed. All experiments used the cells between P5 and P10.

Lineage Differentiation

Lineage differentiation was performed using a protocol adapted from that published previously.[34] Cells were cultured as monolayers in EM for 4 days followed by culture in DM for 4 days to initiate cell differentiation. Both EM and DM were changed every 48 hours. DM did not contain growth factors (Wnt-3A, R-spondin, or noggin). Sodium butyrate (B; 5 mmol/L, 263190050; Acros Organics, Waltham, MA), γ-secretase inhibitor DAPT (N-[(3,5-Difluorophenyl)acetyl]-L-alanyl-2-phenyl]glycine-1,1-dimethylethyl ester; 10 μmol/L, M60023-5; Xcessbio, San Diego, CA) were added as indicated to induce differentiation into either absorptive colonocytes or mucus-producing goblet cells.

Microfabrication and Surface Modification of Polydimethylsiloxane Stamps

Polydimethylsiloxane (PDMS) stamps were used to micromold collagen scaffolds with an array of microwells. The PDMS stamps possessed an array of microposts with slanted walls and rounded top surfaces (height, 430 μm; base diameter, 125 μm). A custom-formulated 1002F epoxy photoresist was used to generate high-aspect ratio microposts. Formulation of 1002F photoresist was described in a previous publication.[35] A film of 1002F photoresist of 150-μm thickness was created on a glass slide by spin-coating 1002F photoresist (formulation 100) on a glass slide (75 mm × 50 mm × 1 mm; Corning). After baking at 95°C for 60 minutes, a second layer of 1002F of 150-μm thickness was spin-coated on the top of the first layer. After baking at 95°C for 60 minutes, a third layer of 1002F of 130-μm thickness was spin-coated on the top of the second layer. The film (total thickness, 430 μm) was baked at 95°C for 60 minutes to evaporate the solvent. To create the sloped post sidewall, the film was exposed to UV light at a dose of 1500 mJ/cm^2 from the backside (ie, through the glass slide). A post-exposure baking was next performed in a 95°C oven for 10 minutes followed by baking on a 120°C hotplate for 10 minutes. The resist then was developed with propylene glycol monomethyl ether acetate for 60 minutes, and baked on a 120°C hotplate for 60 minutes to harden the film. PDMS stamp 1 was created from the earlier 1002F master mold by spreading PDMS prepolymer on the mold followed by degassing under a vacuum. PDMS on the mold was baked in a 95°C oven for 30 minutes followed by demolding. The demolded PDMS possessed an array of microwells. The PDMS mold was treated with plasma for 2 minutes, and coated with octyltrichlorosilane using a vapor-phase process for 16 hours. A second PDMS stamp (stamp 2) was replicated in the same manner from stamp 1 to create a negative replica with an array of posts with slanted sides.

The PDMS stamps were coated with poly(ethylene glycol) to eliminate collagen adhesion during micromolding. The PDMS stamps were surface-grafted with poly(ethylene glycol) as described previously using UV-mediated graft polymerization.[36] Briefly, PDMS stamps were placed in a glass tube with a screw-cap (GL 25, polytetrafluoroethylene [PTFE] protected seal; Schott, Elmsford, NY). The tube was filled with a mixture of 10 wt% poly(ethylene glycol) methyl ether acrylate monomer (454990; Sigma-Aldrich, St. Louis, MO), 0.5 mmol/L sodium periodate (311448; Sigma-Aldrich), 0.5 wt% benzyl alcohol (108006; Sigma-Aldrich) in water. The tube then was exposed to UV radiation in a Loctite 7411-S UV Flood System (Henkel, Düsseldorf, Germany) for 4 hours. The stamps then were rinsed with deionized water and incubated in deionized water overnight to remove noncovalently attached polymer and monomer. The grafted stamps were stored in 75% ethanol until use.

Micromolding Collagen Scaffolds on a Modified Transwell Insert

A cross-linked collagen scaffold possessing microwell structures was micromolded on the top of a porous membrane in a modified 12-well Transwell insert (3401; Corning, Tewksbury, MA) using a PDMS stamp. To construct the modified insert, the polycarbonate porous membrane was removed from the Transwell insert using sandpaper. Next, a hydrophilic PTFE porous membrane (BGCM00010; Millipore, Burlington, MA) was attached to the insert using a biocompatible transfer adhesive (1504XL; 3M, Moncure, NC). To reduce the effective area of the porous membrane (ie, from 12-mm diameter to 3-mm diameter), the backside of the porous membrane was blocked by attaching a nonpermeable cyclic olefin copolymer plastic film (4-mL thick, TOPAS 6013; TOPAS Advanced Polymers, Florence, KY).

Collagen in the absence of acetic acid was used for micromolding because the acetic acid (low pH) interfered with the cross-linking reaction. Acetic acid was removed by freeze drying the collagen solution (20 mmol/L acetic acid) on a lyophilizer for 72 hours, followed by redissolving the dried collagen solid in 2-(N-morpholino)ethanesulfonic acid buffer (0.1 mol/L, pH 5) to generate a 5 mg/mL collagen solution. Collagen solution (400 μL), 600 mmol/L 1-ethyl-3-(3-dimethylaminopropyl)carbodiimide hydrochloride (EDC; 50 μL), and 150 mmol/L N-hydroxysuccinimide (NHS; 50 μL) were mixed in a conical tube on ice by pipetting up and down 40 times. The trapped air bubbles in the mixture were removed by centrifugation at 3000×g for 1 minute. The modified Transwell inserts were placed in a 12-well plate. Collagen mixture (50 μL) was added to the center of the Transwell insert, and a PDMS stamp was placed on the top of the mixture. (Note that the mixture starts to gel within 5 minutes upon mixing the collagen with EDC and NHS. Thus, the earlier-described steps must be completed within 5 minutes.) To remove the trapped air bubbles among the microposts of the PDMS stamp, the 12-well plate was placed inside a pressure pot (448PP; Dental Planet, Wichita Falls, TX), and pressurized to 40 psi using nitrogen for 2 hours. After removal of the plate from the pot, the insert was incubated in deionized water, and the PDMS stamp was demolded from the solidified collagen scaffold. The collagen scaffold was incubated in 2 L of deionized water for 24 hours to remove residual EDC/NHS. The scaffolds were sterilized with 75% ethanol for 5 minutes, rinsed with PBS for 5 minutes 3 times, and stored in PBS at 4°C until use.

Characterization of Chemical Gradients Applied Across the Scaffold

An impermeable plastic film was attached to the porous membrane on the side opposite to the scaffold to reduce the available area for transport across the membrane from 113 mm^2 (standard 12-well Transwell size) to 7 mm^2. The film decreased the area available for diffusion so that upper and lower reservoirs could be approximated as an infinite source and sink. To characterize the chemical gradient profile over time, 100 μg/mL of fluorescein-dextran (molecular weight, 40 kilodaltons) was added either to the top compartment (0.5 mL) or to the bottom compartment (1.5 mL). PBS then was added to the other compartment (bottom compartment, 1.5 mL; top compartment, 0.5 mL). The fluorescein-dextran concentration was measured at 24, 48, and 72 hours in the compartment originally filled with PBS.

Generating In Vitro Crypts

In vitro crypts were formed by culturing cells on the micromolded scaffolds followed by application of a chemical gradient across the scaffold. Before plating cells on the micromolded collagen scaffold, the scaffold was coated with 10 μg/mL human collagen (5007-20ML; Advanced Biomatrix, San Diego, CA) in PBS at 37°C overnight. The scaffold was rinsed with 2 mL PBS. Monolayers of primary cells were expanded on the neutralized collagen hydrogel in a 6-well plate as described earlier in the "Monolayer Culture on a Neutralized Collagen Hydrogel" section. When the monolayers reached >80% confluency, the monolayer was detached from the collagen by incubation with collagenase and then fragmented by EDTA and mechanical agitation as described earlier. The cells then were plated on the top surface of the micromolded collagen in the modified Transwell insert. Cells from 1 well of the 6-well plate were dispersed into 4 separate modified 12-well Transwell inserts. The cells were cultured in 3 mL EM per well (1 mL in the top compartment, and 2 mL in the bottom compartment), and the medium was exchanged every 48 hours. When the cells covered the entire surface of the scaffolds, typically approximately 7 days, a gradient of growth factors was applied across the shaped collagen scaffold and cells. DM (0.5 mL) was placed into the top compartment, and SM (1.5 mL) was added into the bottom compartment. The DM and SM were changed daily to maintain a stable gradient across the collagen scaffold or long axis of the in vitro crypt. Typically, polarization of the in vitro tissue was observed in 4 days under these chemical gradient conditions. When maintained under this chemical gradient, the polarized tissue was maintained for up to 32 days (the longest time tested). To assay the impact of other chemical gradients on crypt polarity, short-chain fatty acids (SCFAs) or cytokines (100 ng/mL tumor necrosis factor-α (TNF-α) [300-01A; Peprotech] and 10 ng/mL interferon-γ (IFN-γ) [300-02; Peprotech]) were added to either the top or bottom compartment as indicated.

Simultaneous Assay of 5-Ethynyl-2-Deoxyuridine Incorporation, Alkaline Phosphatase Activity, Mucin 2 Presence, and DNA Content

Living cells were pulsed with 5-ethynyl-2-deoxyuridine (EdU) and assayed for alkaline phosphatase (ALP). The cells then were fixed and sequentially stained for EdU incorporation (S-phase cells), mucin 2, and DNA. Cells were first pulsed with 10 μmol/L of EdU for 24 hours at 37°C, rinsed with PBS, and incubated with a red ALP substrate (SK-5100; Vector Laboratories, Burlingame, CA) in Tris buffer (0.15 mol/L, pH 8.4) for 30 minutes at 37°C. The cells were rinsed with PBS, fixed in 4% paraformaldehyde for 15 minutes, and permeabilized with 0.5% Triton X-100 in PBS for 20 minutes. Incorporated EdU was labeled with Click-iT EdU Alexa Fluor 647 (C10340; ThermoFisher). The cells were then rinsed with 0.75% glycine in PBS for 5 minutes 3 times, followed by blocking with 10% donkey serum (017-000-121; Jackson Immunoresearch, West Grove, PA) for 1 hour. The cells were incubated in rabbit mucin 2 (Muc2) antibody (1:200, sc-15334; Santa Cruz Biotechnology, Dallas, TX) at 4°C overnight, and stained with donkey anti-rabbit IgG-conjugated Alexa Fluor 488 (1:500, 711-545-152; Jackson Immunoresearch) for 45 minutes. Finally, the DNA was stained with Hoechst 33342 (2 μg/mL, B2261; Sigma-Aldrich) for 15 minutes.

Quantification of Mucin Secretion and ALP Activity

The protein level of Muc2 secreted by the cells into the supernatant was determined quantitatively by a direct enzyme-linked immunosorbent array (ELISA) adapted from a previous publication.[37] Cells were incubated for 48 hours and their supernatant collected and diluted with coating buffer (0.1 mol/L sodium carbonate, pH 9.5) at a ratio between 1:10 and 1:100, and 100 μL was added to each well of an ELISA plate (15042; ThermoFisher). The plate was incubated in a 40°C oven overnight to let the samples dry. The wells then were washed 3 times with 200 μL PBS, blocked with 200 μL of 1% bovine serum albumin (BSA) (A9647; Sigma) in PBS for 1 hour at room temperature, and incubated with 100 μL of horseradish peroxidase (HRP)-conjugated MUC2 primary antibody (sc-515032; Santa Cruz Biotechnology; diluted in 1% BSA to 15 ng/mL) for 16 hours at 4°C. The wells then were washed 5 times with 200 μL of 0.05% Tween-20 in PBS. SuperSignal ELISA Femto horseradish peroxidase substrate (37075; ThermoFisher; 10× dilution in deionized water, 100 μL) was added to each well. After 10 minutes, the luminescence was measured using a plate reader (SpectraMax M5; Molecular Devices, Sunnyvale, CA). Media from wells without cells were used as a control. The results are expressed as a percentage of the control medium and were normalized to the total protein content of the cells from which the supernatant was collected.

To measure the ALP enzymatic activity, the cells were detached from the collagen hydrogel by incubation in collagenase for 15 minutes at 37°C as described in a previous section, and washed twice with 5 mL PBS. The cell pellets were lysed with 200 μL lysis buffer (1% Triton X-100, 150 mmol/L KCl, 50 mmol/L HEPES, 5 mmol/L EDTA, 5% glycerol), vortexed, and incubated on ice for 20 minutes. After centrifugation at 10,000×g (10 min, 4°C), the supernatants were collected to quantify ALP activity and the total protein content. The ALP activity of the cell lysates was measured using the Sensolyte luminescent ALP assay (AS-72122; Anaspec, Fremont, CA). ALP from calf intestine was used as a positive control and standard. The protein concentration of the cell lysates was measured by a Pierce is now a ThermoFisher trademark, not a company. There is no need to provide address for Pierce BCA protein assay (23225; ThermoFisher). The ALP activity is expressed as picograms equivalent to the calf intestine standard and normalized to the cell protein amount. Three wells were used for the measurements of both mucin secretion and ALP activity (n = 3).

Immunofluorescence Staining

Immunofluorescence was used to show the presence of different cell types and subcellular structures of a tissue (eg, biopsies, monolayers, organoids, in vitro crypts). To obtain tissue slices, the specimen was first fixed in 4% paraformaldehyde for 15 minutes, rinsed with PBS, and incubated in 30% sucrose at 4°C overnight. The tissue then was embedded in a cryo-embedding optimal cutting temperature (OCT) medium (Tissue-Tek O.C.T. Compound, VWR, Radnor, PA), and the frozen tissue block was sectioned into 10-μm–thick films by a cryostat. For zonula occludens-1 (ZO-1), E-cadherin, occludin, and β-catenin, the cells were fixed with ice-cold methanol and placed at -20°C for 15 minutes. To preserve mucins for Muc2 staining on in vitro crypts, the tissue was fixed with Carnoy's solution (90% methanol and 10% acetic acid) for 30 minutes. For immunostaining, the primary antibodies used were antibodies to olfactomedin-4 (Olfm4) (1:500, 14369; Cell Signaling Techology, Danvers, MA), cytokeratin 20 (KRT20) (1:500, 60183-1-lg; ProteinTech), Muc2 (1:200, sc-15334; Santa Cruz Biotechnology), ezrin (1:200, PA5-17518; ThermoFisher), integrin β4 (1:200, sc-9090; Santa Cruz Biotechnology), ZO-1 (1:100, 21773-1-AP; Proteintech, Rosemont, IL), β-catenin (1:200, sc-9090; Santa Cruz Biotechnology), occludin (1:100, 13409-1-AP; Proteintech), and E-cadherin (1:100, 20874-1-AP; Proteintech). Antigen retrieval was performed when specimens were stained for Oflm4 and KRT20. For other stains, antigen retrieval was not required to visualize immunofluorescence staining. For antigen retrieval, the specimen sections were rinsed with PBS 3 times to remove the cryo-embedding OCT medium. The slides were placed in a retrieval solution (RV1000MMRTU, Reveal Decloaker; Biocare Medical, Pacheco, CA) in a plastic Coplin jar in a 95°C water bath for 15 minutes. The jar then was placed at 20°C for 15 minutes. The sections with and without antigen retrieval then were rinsed with PBS and blocked with 10% donkey serum for 1 hour at 20°C. The sections were incubated with primary antibodies overnight at 4°C. The sections then were stained with secondary antibody, donkey anti-rabbit, or mouse IgG conjugated with Alexa Fluor 488 or 594 (1:500, 711-585-152 or 715-585-150; Jackson Immunoresearch). The nuclei were stained with Hoechst 33342 (2 μg/mL) for 15 minutes.

Electron Microscopy

For scanning electron microscopy (SEM), samples were dried with a critical point dryer (PVT-3, Tousimis Semidri, Rockville, MD), coated with 10-nm metal by a sputter coater (Cressington 108, Cresington Scientific Instruments, Watford, UK), and inspected by a SEM (FEI Quanta 200 ESEM; FEI Company, Hillsboro, OR).

Fluorescence Microscopy

Specimens were imaged using a Nikon Eclipse TE300 inverted epifluorescence microscope (Nikon, Melville, NY) equipped with 4′,6-diamidino-2-phenylindole/fluorescein isothiocyanate/Texas Red/Cyanine 5 (CY5) filter sets. Images were acquired at randomly selected locations within a specimen using a 10× (N.A. numerical aperture (N.A.) = 0.3) or 4× (N.A. = 0.13) objective. S-phase cells stained with EdU were imaged using a CY5 filter (excitation filter, 604–644 nm; emission, 672–712 nm), ALP stain was imaged with a Texas Red filter (excitation filter, 542–582 nm; emission, 604–644 nm), Muc2 immunofluorescence was visualized with a fluorescein filter (excitation filter, 450–490 nm; emission, 520 nm long pass), and DNA stained by Hoechst 33342 was identified using a 4′,6-diamidino-2-phenylindole filter (excitation filter, 352–402 nm; emission, 417-477 nm).

Confocal microscopy was performed using a confocal laser scanning microscope (Fluoview FV3000; Olympus, Waltham, MA) with laser-based excitation and emission wavelengths selected using a holographic transmission diffraction grating.

Image Analysis

Images were empirically thresholded using ImageJ software (https://imagej.nih.gov/ij/). ImageJ also was used to quantitatively measure the monolayer surface area possessing suprathreshold fluorescence for the EdU, ALP, or Muc2 stains. The identified surface area then was divided by the total cell area calculated from the image area positive for Hoechst fluorescence (DNA stain) and expressed as a percentage cell area positive for the EdU, ALP, or Muc2 stain. All data used 5 randomly selected locations of the same monolayer ($n = 5$), and the average with a single SD is shown unless otherwise specified.

Statistics

Statistical analysis was performed using a 1-way analysis of variance followed by a multiple comparison test with the Tukey honest significant difference procedure conducted at the 5% significance level. All analyses of variance returned P values less than .004. Multiple comparison testing was performed on all pairwise comparisons between experimental groups. Analyses of variance and subsequent multiple comparisons were performed using MATLAB (MATLAB 2014b; The MathWorks, Inc, Natick, MA). An unpaired 2-tailed Student t test was used to compare the outcomes from 2 experimental conditions in the cytokine perturbation experiment.

All authors had access to the study data and reviewed and approved the final manuscript.

Imaging and Assay of Whole Crypts Detached From the In Vitro Tissue

Before removal from the tissue, the crypts were stained as described earlier for EdU incorporation, ALP activity, Muc2 presence, or DNA content. To assess the polarity of the in vitro crypts, a side view of the intact crypts was obtained by scraping the crypts loose from the tissue and scaffold using a tungsten dissecting needle (RS-6063; Roboz Surgical Instrument Co, Gaithersburg, MD). Detached crypts were overlaid onto a glass slide onto which they settled, lying in a horizontal position. The crypts then were imaged using standard fluorescence microscopy. The position of proliferating cells (EdU$^+$) along the basal–luminal crypt axis was obtained by evenly dividing the crypt into 8 regions. The fluorescence intensity ratio of the EdU stain relative to that of Hoechst fluorescence (DNA) from each region was obtained by ImageJ. The EdU/Hoechst ratio then was plotted against position along the basal–luminal crypt axis. Twenty crypts were quantified under identical fluorescence measurement conditions.

To assay the impact of SCFAs or cytokines on the polarity of in vitro crypts, the crypts were scraped from the array and imaged as described earlier. The number of S-phase cells per crypt was obtained by manually counting the number of EdU$^+$ cells per crypt using ImageJ. The relative proliferation length (expressed as a percentage) is defined as the length of the crypt possessing EdU+ cells divided by the total length of the crypt. The normalized ALP activity of the crypts was obtained by measuring the total fluorescence intensity of the ALP stain divided by the fluorescence intensity of the Hoechst DNA stain. More than 10 crypts were quantified for each data point under identical imaging conditions.

Unless otherwise specified, the data shown for a single experiment used crypts or cells obtained from a single biopsy (male; age, 52 y). Experiments used material from biopsy specimens from 3 different human beings and the results were consistent over time without outliers. Data from representative experiments are presented.

Results

Organoid Culture of Human Colonic Epithelial Cells

The luminal surface of the human colonic epithelium possesses a high density of crypts or invaginations interspersed among luminal columnar cells (Figure 1*A*). Between these cell-covered invaginations lies a lamina propria that shapes and supports the crypt and its cells. Proliferative stem/progenitor cells (Olfm4$^+$) are confined to the basal side of the crypts, while the nondividing differentiated cells are located at the luminal surface.[38,39] This exquisite tissue polarity with compartmentalization of proliferative and differentiated cells is thought to be maintained in vivo by a gradient of well-balanced growth signals (Wnt-3A, Notch, bone morphogenic protein [BMP], and other factors) spanning the long axis of crypt from the luminal to the basal region.[40] This microenvironment also ensures the unidirectional migration of cells from the proliferative to the differentiated cell zone so that the luminal epithelial cells are replaced every 5–7 days.[41] The U shape of the crypt permits the stem cells to be in a contiguous monolayer with their differentiated progeny while surrounded by a chemical microenvironment distinct from that of their differentiated offspring. The growth-factor–rich microenvironment supports the stem cells as they proliferate and protects these cells from the harsh milieu found within the colonic lumen.[42] Isolation of crypts from the colon and placement within a Matrigel patty with appropriate supporting growth

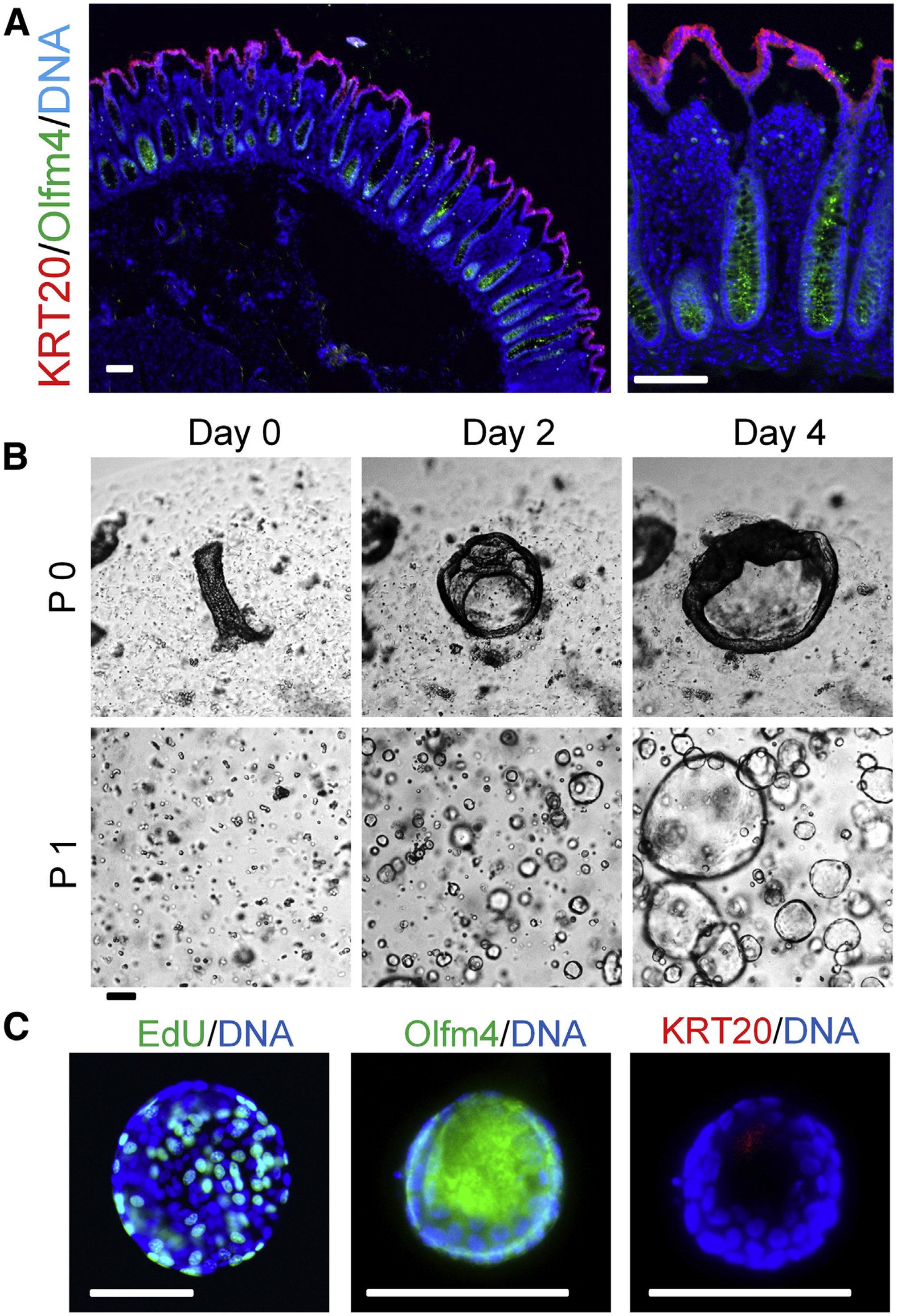

Figure 1. Organoid culture of human colonic epithelial cells. (*A*) Immunofluorescence staining of human colonic tissues. A fluorescence image of tissue immunostained for KRT20$^+$ (red) and Olfm4$^+$ (green) is shown. DNA was stained with Hoechst 33342 (blue). (*B*) Human colonic organoids embedded in Matrigel using a crypt as the starting material. The brightfield images on days 0, 2, and 4 of culture at passage numbers 0 and 1 are shown. (*C*) EdU pulse labeling and immunofluorescence staining (Olfm4 and KRT20) of organoids after 4 days in culture. DNA was stained with Hoechst 33342. *Scale bars*: 100 μm.

factors enables the stem cells to proliferate but with transition into a single-layered, hollow organoid, with loss of the crypt anatomic features (Figure 1*B*).[39] When maintained under a growth-factor–rich medium (EM), the organoids predominantly comprise proliferative cells (EdU$^+$, Olfm4$^+$), with a paucity of differentiated cells (KRT20$^+$) (Figure 1*C*). The loss of tissue polarity likely is owing to the absence of a polarity-defining growth factor gradient within the surrounding hydrogel as well as the inability of the Matrigel to guide the growing organoids into the proper sized and shaped crypt structures.[22,25] Although the Matrigel-based organoid system has been an enabling technology for experimentation into intestinal stem cell behavior and the creation of many intestinal disease models, the system does not fully recapitulate the architecture and physiology of in vivo crypts. The organoid morphology and surrounding hydrogel remain incompatible with many desired investigations, especially those focusing on crypt dynamics or studying exposure to organisms and chemicals selectively impacting one face (luminal or basal) of the intestinal epithelium.

Monolayer System Allows Self-Renewal and Differentiation of Human Colonic Epithelial Cells in Response to External Biochemical Cues

Wang et al[25] recently developed a collagen hydrogel scaffold that supported a self-renewing monolayer of human colonic epithelial cells with both stem/proliferative cells as well as the various differentiated cells (goblet cells, enteroendocrine cells, and colonocytes). Under the reported growth-factor–rich culture conditions, both monolayers on collagen and organoids within Matrigel predominantly comprised proliferative cells, with a minority of differentiated cells.[25] Prior reports have shown that the stem/proliferative cells of organoids can be chemically differentiated into either absorptive cells or goblet cell lineages by modulating Wnt and Notch signals.[34] To determine whether the monolayer cells also might be force differentiated, the monolayers were cultured in EM for 4 days and then to media promoting differentiation for 4 days: SM (with growth factors but without inhibitors/hormones), DM (without growth factors, inhibitors/hormones), DM plus 5 mmol/L butyrate (DM-B), or DM plus 10 μmol/L DAPT (DM-D) (Figure 2*A* and *B*). Cells remained proliferative in SM owing to the presence of growth factors, but grew at a slower rate relative to cells in EM (Figure 2*B* and *E*). Cell proliferation largely was eliminated in DM as evidenced by a decrease in S-phase cells as a result of the absence of growth factors. However expression of differentiation markers (ALP$^+$ for colonocytes, Muc2$^+$ for goblet cells) increased relative to that of cells in SM (Figure 2*B* and *E*). Addition of butyrate to DM increased ALP activity but not Muc2 expression, suggesting that the monolayers predominantly comprised absorptive colonocytes (Figure 2*B* and *E*). Butyrate is produced in vivo by bacterial fermentation of fiber

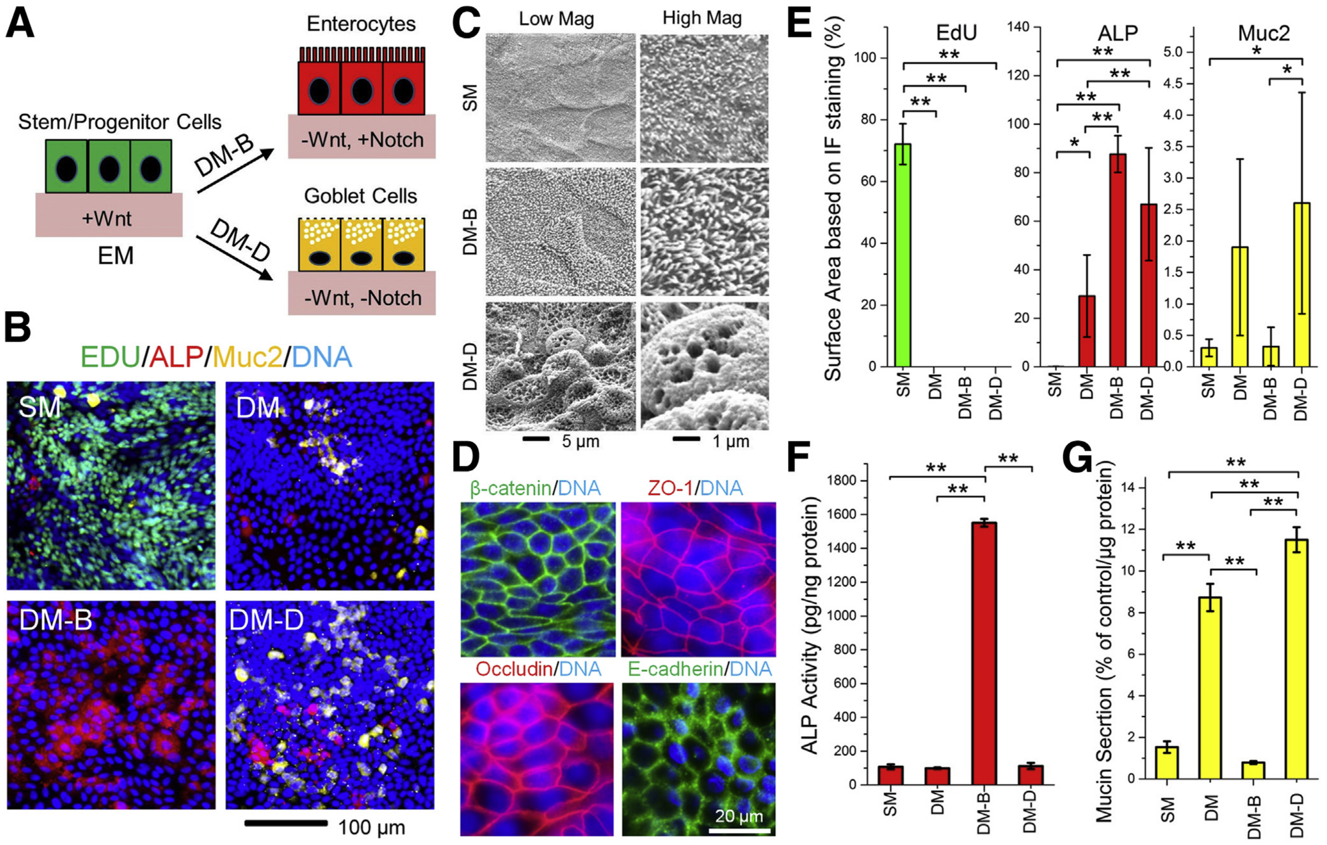

Figure 2. Forced differentiation of human colonic epithelial cells grown as a monolayer. (*A*) Schematic showing the forced differentiation of the cells. Cells were cultured in expansion medium (EM) for 4 days and then either stem medium (SM) or differentiation medium (DM) for 4 days. Additional molecules added to the DM were 5 mmol/L butyrate (DM-B) or 10 μmol/L DAPT (DM-D). (*B*) Fluorescence microscopy of monolayers grown under the different differentiation media. Colors as follows: EdU, green; ALP, red; Muc2, yellow; DNA, blue. (*C*) Apical surface topography of human colonic monolayers inspected by SEM. *Left*: low-power magnification; right panels, high power magnification. (*D*) Immunofluorescence staining of epithelial monolayers (6 days in expansion medium) using antibodies directed against β-catenin (green), ZO-1 (red), occludin (red), and E-cadherin (green). Nuclei were stained with Hoechst 33342 (blue). (*E*) The percentage of the monolayer surface area showing fluorescence from the EdU, Muc2, and ALP stains under the various culture conditions. (*F*) ALP activity of cell lysates under the various culture conditions. (*G*) Mucin secretion by the monolayer under the various culture conditions. IF, immunofluorescence; Mag, magnification. $^*P < .05$ and $^{**}P < .005$.

and is thought to act as a Notch activator.[43,44] In contrast, DAPT, a Notch inhibitor, increased Muc2 expression, suggesting that Notch inhibition increased Goblet cell production under these conditions.[43,44] These results were consistent with the apical morphology of the monolayers when inspected by SEM (Figure 2*C*): proliferative cells

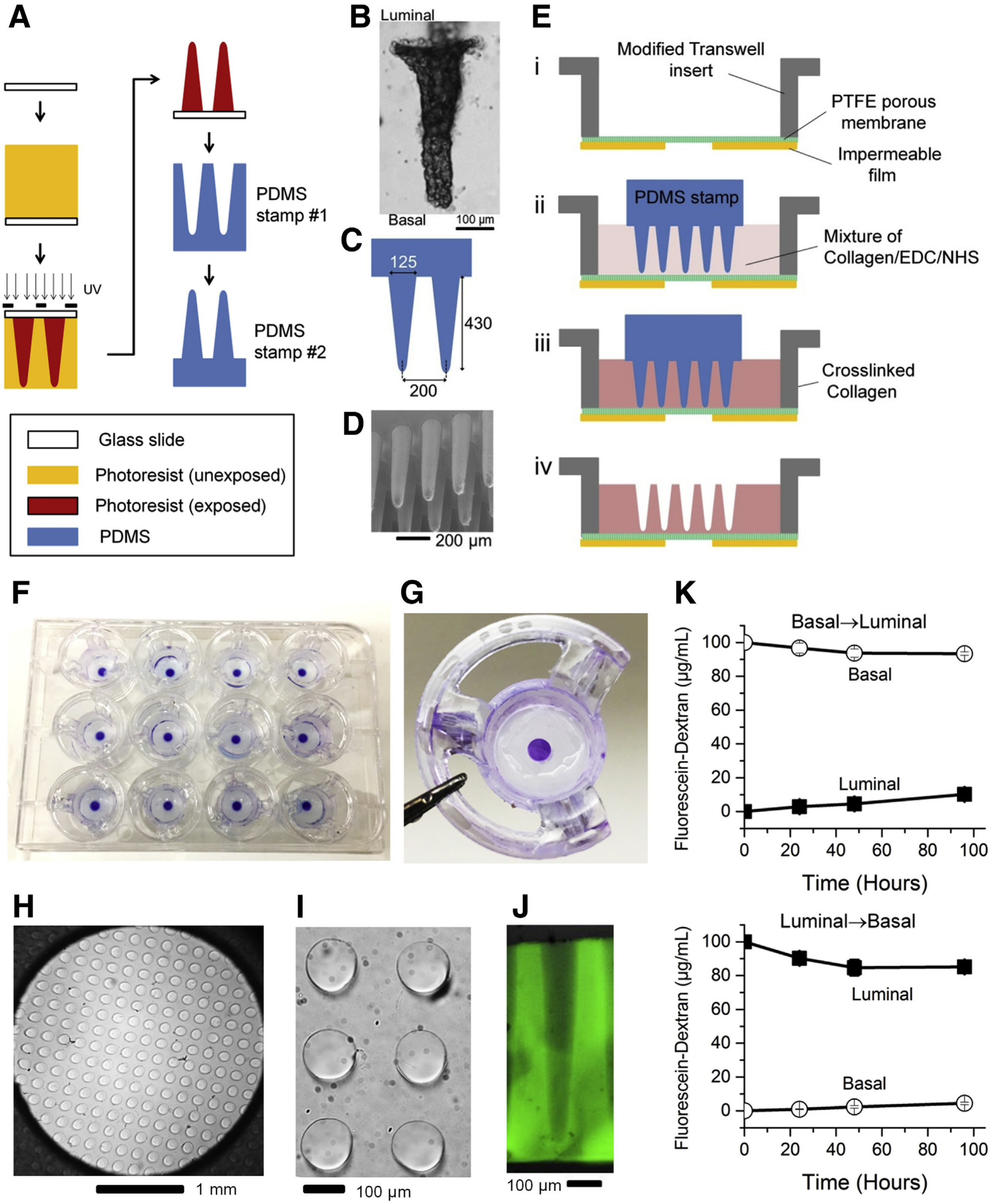
A
UV
PDMS stamp #1
PDMS stamp #2
Glass slide
Photoresist (unexposed)
Photoresist (exposed)
PDMS
B
Luminal
Basal
100 μm
C
125
430
200
D
200 μm
E
i
Modified Transwell insert
PTFE porous membrane
Impermeable film
ii
PDMS stamp
Mixture of Collagen/EDC/NHS
iii
Crosslinked Collagen
iv
F
G
H
1 mm
I
100 μm
J
100 μm
K
Basal→Luminal
Basal
Luminal
Fluorescein-Dextran (μg/mL)
0
20
40
60
80
100
Time (Hours)
Luminal→Basal
Luminal
Basal
Fluorescein-Dextran (μg/mL)
Time (Hours)

(under SM) showed a low density of stunted microvilli and no visible secretory granules, colonocytes (under DM-B) showed a high density of long microvilli but again without visible secretory granules, and goblet cells (under DM-D) showed secretory granules lining their apical surfaces but without microvilli. In addition, tight junction proteins (β-catenin, ZO-1, occludin, and E-cadherin) were expressed in the monolayers (Figure 2*D*), suggesting that this can be optimized to interrogate barrier function.

The presence of ALP activity and Muc2 was spatially heterogeneous in the monolayers, which led to a large variability in their detection when measured by fluorescence microscopy (Figure 2*B* and *E*). For this reason, ELISA and enzymatic assays able to measure the ALP activity and Muc2 presence from the entire monolayer also were performed. ALP enzymatic activity in the presence of DM-B was significantly greater than that for monolayers incubated with SM, DM, or DM-D, again suggesting that the DM-B monolayer was primarily colonocytes and that Notch activation drove colonocyte formation under these conditions (Figure 2*F*). Muc2 secretion was increased significantly by incubation in DM-D relative to that of DM, and both of these media yielded substantially more Muc2 than incubation in either SM and DM-B (Figure 2*G*). Notch inhibition under these conditions enhanced the formation of Goblet cells and mucin presence in the monolayer cultures (Figures 2*B* and 4*M*). These data taken together suggest that cells in the monolayer behave in a similar fashion to those in the organoids in response to external biochemical cues.[34] Thus, the collagen hydrogel scaffold is a suitable matrix for culture of proliferative monolayers or differentiated human colonic epithelial cells. The ability to redirect monolayer cell fate into either of the 2 differentiated lineages provides additional evidence for the presence of malleable stem cells within the monolayers.

Microfabrication of a Collagen Scaffold to Support Chemical Gradients

To shape the monolayers into the architecture of in vivo human colon crypts, we micromolded collagen hydrogels on a porous membrane using a PDMS stamp (Figure 3*A–E*). A hydrophilic, 0.4-μm PTFE membrane was selected because of its optical transparency, low fluorescence, and high permeability. The stamps possessed an array of high-aspect ratio posts with a slanted sidewall and rounded end (Figure 3*A*, *C*, and *D*). During the molding process, the PDMS stamp with posts was pressed into the collagen to create microwells with a size and shape similar to that of the human colon crypts (Figure 3*E* and *H–J*). To strengthen the collagen scaffold and prevent cells from deforming the microwells, the collagen was mixed with EDC/NHS to initiate collagen cross-linking during the molding process.[45] The micromolded collagen scaffold possessed 245 microwells in the central 7 mm^2 area of a modified 12-well Transwell insert (Figure 3*F–J*). The Transwell platform was used because of the ease in which a gradient could be initiated across the long axis of the microwells (z-axis of the scaffold) (ie, simply placing different media in the basal and luminal reservoirs). The platform also can be adapted to other chamber types (such as Seahorse Metabolic Analyzer, Agilent, Santa Clara, CA) by modifying the insert design.

To determine the period of time over which the basal and luminal reservoirs could act as an infinite source and sink to support a stable gradient of growth factors across the collagen scaffold, the diffusion of a model compound, fluorescein-dextran, across the scaffold/membrane was measured (Figure 3*K*). Fluorescein-dextran (40 kilodaltons) was chosen because it is of similar molecular weight to Wnt-3A (39.7 kilodaltons), R-spondin (40.0 kilodaltons), and noggin (46 kilodaltons). At 0 hour, the fluorescein-dextran concentration was (source) = 100 μg/mL and (sink) = 0 μg/mL. At 24 hours, when the basal reservoir was the source, the concentration was (source) = 96.6 ± 3.0 μg/mL and (sink) = 2.9 ± 0.7 μg/mL (luminal reservoir). When the direction of diffusion was reversed (ie, the basal reservoir was now the sink), the (sink) = 0.9 ± 0.2 μg/mL and the (source) = 90.2 ± 0.9 μg/mL (luminal reservoir). These data suggested that a stable, steep chemical gradient was established across the collagen scaffold when the fluids in the basal and luminal reservoirs were replenished every 24 hours.

Construction of Polarized Colonic Crypts

Colonic crypts were constructed by growing cells on the collagen scaffold until the cells covered the surface including that of the sides and bottoms of the microwells (Figure 4*A*). When cultured in the presence of EM, which promotes rapid cell proliferation, the cells typically covered

Figure 3. (***See previous page***). **Scaffolding and gradient cassette for the culture of in vitro crypts.** (*A*) Fabrication process for the PDMS stamps used to micromold collagen scaffolds mimicking the topography of epithelium of human colon. (*B*) Transmitted light microscopy of a human colonic crypt from a biopsy sample. (*C*) Geometry of the PDMS stamp that was used to micromold collagen. Units are shown in micrometers. (*D*) SEM image of the PDMS stamp. (*E*) Schematic of the micromolding process used to generate a shaped, cross-linked collagen scaffold on a modified Transwell insert. (*F*) Image of the 12 scaffolds within a 12-well plate. To show the trans-scaffold transport occurred only at the central area, the insert was briefly exposed to 0.1% toluidine blue from the basal side. The toluidine blue only stained the scaffold within the central 3-mm diameter area in contact with the basal compartment. (*G*) Image of a single scaffold within an insert. (*H*) Top view of an array of microwells created in the scaffold. (*I*) Close-up view of a region of the scaffold in panel H. (*J*) Side view of a cross-section through a fluorescein-labeled collagen scaffold. (*K*) Concentration of fluorescein dextran (molecular weight, 40 kilodaltons) measured at the luminal (*solid squares*) and basal (*empty circles*) compartments at 24, 48, and 72 hours. *Top plot*: Diffusion from basal to luminal. At 0 hours, 0.5 mL PBS was added to the luminal compartment and 1.5 mL fluorescein dextran (100 μg/mL) was added to the basal compartment. *Bottom plot*: Diffusion from luminal to basal. At 0 h, 0.5 mL fluorescein dextran (100 μg/mL) was added to the luminal compartment and 0.5 mL PBS was added to the basal compartment.

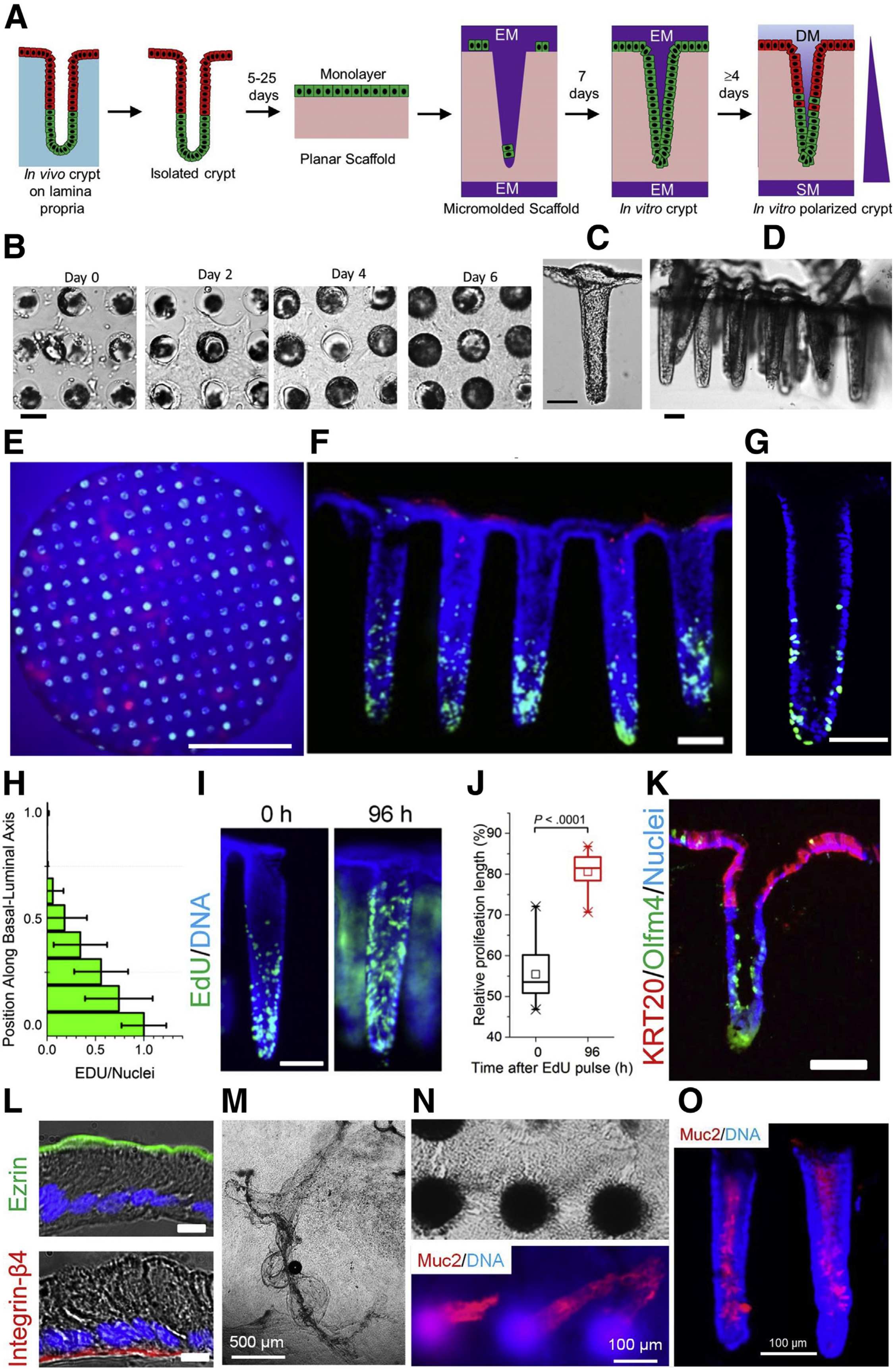
A
In vivo crypt on lamina propria
Isolated crypt
5-25 days
Monolayer
Planar Scaffold
EM
EM
Micromolded Scaffold
7 days
EM
EM
In vitro crypt
≥4 days
DM
SM
In vitro polarized crypt
B
Day 0
Day 2
Day 4
Day 6
C
D
E
F
G
H
1.0
0.5
0.0
Position Along Basal-Luminal Axis
0.0
0.5
1.0
EDU/Nuclei
I
0 h
96 h
EdU/DNA
J
P < .0001
90
80
70
60
50
40
Relative proliferation length (%)
0
96
Time after EdU pulse (h)
K
KRT20/Olfm4/Nuclei
L
Ezrin
Integrin-β4
M
500 μm
N
Muc2/DNA
100 μm
O
Muc2/DNA
100 μm

the scaffolds within 7 days (Figure 4*B*). In contrast to native collagen scaffolds, the cross-linked collagen scaffolds possessed sufficient strength to resist cell-induced deformation of the microwell structures. The crypts within the monolayer could be mechanically dislodged from the scaffolding and placed on a glass slide for microscopy as single crypts or groups of connected crypts (Figure 4*C*–*F*). Each in vitro crypt possessed a shape and dimensions nearly identical to that of the in vivo structures and showed an open luminal end mimicking in vivo crypts.

Polarization of the in vitro crypts was accomplished by adding SM to the basal scaffold side and DM to the luminal scaffold side. SM and DM are identical except that DM does not contain growth factors Wnt-3A, R-spondin, and noggin. Thus, a gradient of growth factors was established along the basal–luminal axis of the crypt structures with the growth factors high at the basal crypt region and low at the luminal epithelial surface (Figure 4*A*). After 4 days of culture under the SM/DM gradient, a polarized in vitro crypt array was created (Figure 4*E*–*G*). Proliferative cells were localized to the base of the microwell or crypt (ie, to the region with high growth factor concentrations), while differentiated, absorptive colonocytes were located on the luminal surface (Figure 4*E*–*G*). Application of a growth factor gradient was sufficient to re-create an asymmetric crypt showing a proliferative and nonproliferative compartment (Figure 4*G* and *H*). Upward cell migration at a rate similar to that occurring in vivo was shown by EdU pulse labeling and tracking the labeled cells over 96 hours as they migrated up the crypt axis (30 μm/day) (Figure 4*I* and *J*).[46] Similar to in vivo crypts (Figure 1*A*), cells of in vitro crypts expressing a differentiation marker (KRT20$^+$) were located at the luminal surface, while cells expressing a marker of colonic stem cells (Olfm4$^+$) were restricted to the basal crypt region, showing a stem cell niche (Figure 4*K*).[38] Goblet cells and mucus also were observed when the cells were cultured for 4 days in EM and 6 days under gradient (Figure 4*M*–*O*). When cells lining the luminal tissue surface (not within the crypt) were immunostained, the cells themselves were asymmetric, displaying properties of an absorptive colonocyte, for example, expressing the microvilli marker ezrin on the cell side adjacent to the media and integrin-β4 on the cell side contacting the collagen scaffold (Figure 4*K* and *L*). The cells also adopted the columnar shape (height, 35 μm; width, 9 μm) typical of differentiated absorptive colonocytes in vivo. When these human in vitro crypts were maintained under a growth factor gradient for 32 days, the epithelium remained as a monolayer, with polarized crypts creating a long-term human epithelial replica.

Response of In Vitro Crypts to Gradients of SCFAs

SCFAs are produced in large quantities by bacterial fermentation of fiber in the colon with the SCFAs such as acetate, propionate, and butyrate present at millimolar concentrations in the lumen.[47] Colonic epithelial cells use these SCFAs as their primary energy source, decreasing the SCFA concentrations near the stem cell compartment to low micromolar concentrations and creating steep SCFA gradients along the length of the crypt.[48,49] The gradient of butyrate (but not acetate or propionate) is thought to play a regulatory role modulating stem cell proliferation by acting as a histone deacetylase inhibitor at low concentration.[48] To assess whether the in vitro tissue was responsive to SCFAs, a gradient of acetate, propionate, or butyrate in addition to that of the growth factors was generated across the in vitro crypts by placing the SCFA into the luminal compartment above the tissue (Figure 5*A*).[47,49,50] The crypts were cultured under the SCFA gradient for 4 days (Figure 5*B* and *C*). All 3 SCFAs increased alkaline phosphatase activity indicative of absorptive colonocytes at the luminal surface, but butyrate was most potent by several fold (Figure 5*C* and *F*). Acetate and propionate gradients did not impact cell

Figure 4. (***See previous page***). **Generation of in vitro human colon crypts.** (*A*) Schematic showing the process of converting in vivo crypts to in vitro crypts. Crypts were isolated from a biopsy, and the cells were expanded as monolayers on a planar scaffold (for 5–25 days, depending on the size of the biopsy specimen and the number of cells banked for other experiments). The cell fragments were cultured on the shaped scaffold for 7 days to create the crypt-like geometry. The cells on the shaped scaffold then were cultured under a biochemical gradient for at least 4 days to polarize the crypts. Differentiated and stem/proliferative cells are shown in red and green, respectively. (*B*) Time-lapse brightfield images showing the growth of cells across the surface of the microwell array. Microwells appeared darker in these brightfield images because their walls were lined with cells. (*C*) Side view of an in vitro–formed crypt. (*D*) Side view of an array of crypts. (*E*) Low-power image (top view) of a 3-mm array under a growth factor gradient. EdU incorporation (green), ALP (red), DNA (blue). (*F*) Fluorescence image (side view) of 5 interconnected in vitro crypts after an EdU pulse (green), ALP stain (red), and Hoechst-DNA labeling (blue). (*G*) A cross-section from a confocal image of a polarized crypt showing the hollow lumen. EdU incorporation (green), DNA (blue). (*H*) Normalized EdU incorporation along the crypt axis. Zero marks the crypt base while 1 denotes 430 μm from the base (crypt top). (*I*) Directional migration of EdU$^+$ cells over time. Images were at 0 and 96 hours after EdU pulse (24-h EdU pulse duration). EdU is green and DNA is blue. (*J*) *Box plots* of the relative proliferation length, which was defined as the length of EdU$^+$ tissue divided by the crypt length (430 μm) at 0 and 96 hours after EdU pulse. Ten crypt units were quantified. $P < .0001$ based on *t* test. (*K*) Cross-section of in vitro crypt immunostained for KRT20 (red) and Olfm4 (green) and DNA labeled with Hoechst 33342 (blue). (*L*) Overlaid brightfield and fluorescence images of cross-sections through the luminal surface between the in vitro crypts. (*M*–*O*) Mucus layer on the tissue. (*M*) A mucus layer was observed above a planar monolayer after fixing the tissue with Carnoy's solution (after 4 days of culture in EM, and 4 days in DM + 10 μm DAPT). (*N*) Mucus was detected within the in vitro crypts (4 days in EM, 6 days under a polarization gradient). *Top*: Brightfield microscopy image. *Bottom*: Immunofluorescence image. Muc2$^+$ mucus protruded from the inside of the crypts up into the media. (*O*) Crypts released from the scaffold were imaged by fluorescence microscopy. (*N* and *O*) Red depicts Muc2 immunofluorescence and blue is Hoechst 33342 fluorescence. *Scale bars*: 1 mm (*E*), 100 μm (*B*–*D*, *F*, *G*, *I*, and *K*), and 10 μm (*L*).

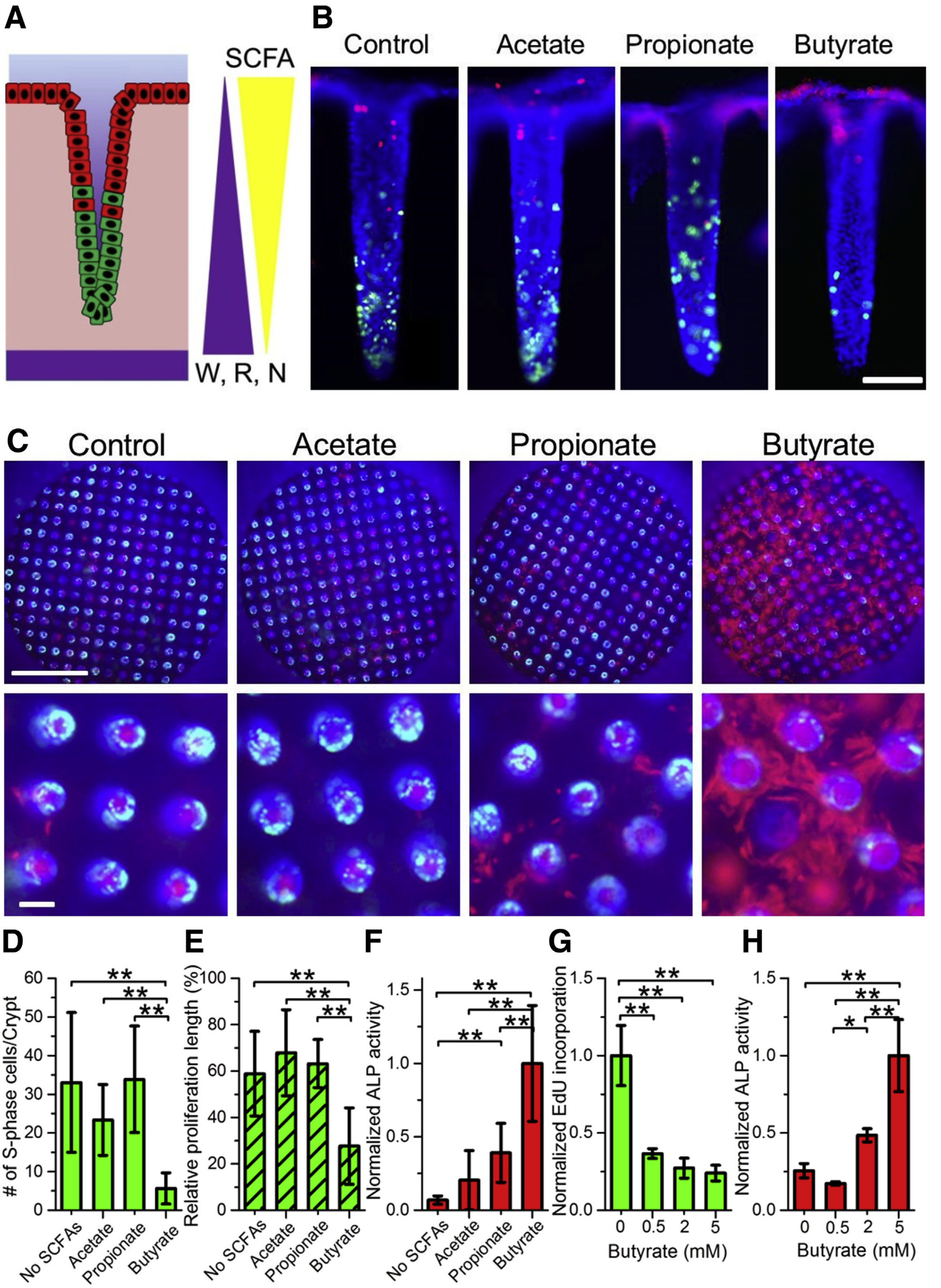
A
SCFA
W, R, N
B
Control
Acetate
Propionate
Butyrate
C
Control
Acetate
Propionate
Butyrate
D
# of S-phase cells/Crypt
0
10
20
30
40
50
60
**
**
**
No SCFAs
Acetate
Propionate
Butyrate
E
Relative proliferation length (%)
0
20
40
60
80
100
**
**
**
No SCFAs
Acetate
Propionate
Butyrate
F
Normalized ALP activity
0.0
0.5
1.0
1.5
**
**
**
**
No SCFAs
Acetate
Propionate
Butyrate
G
Normalized EdU incorporation
0.0
0.5
1.0
1.5
**
**
**
0
0.5
2
5
Butyrate (mM)
H
Normalized ALP activity
0.0
0.5
1.0
1.5
**
**
*
**
0
0.5
2
5
Butyrate (mM)

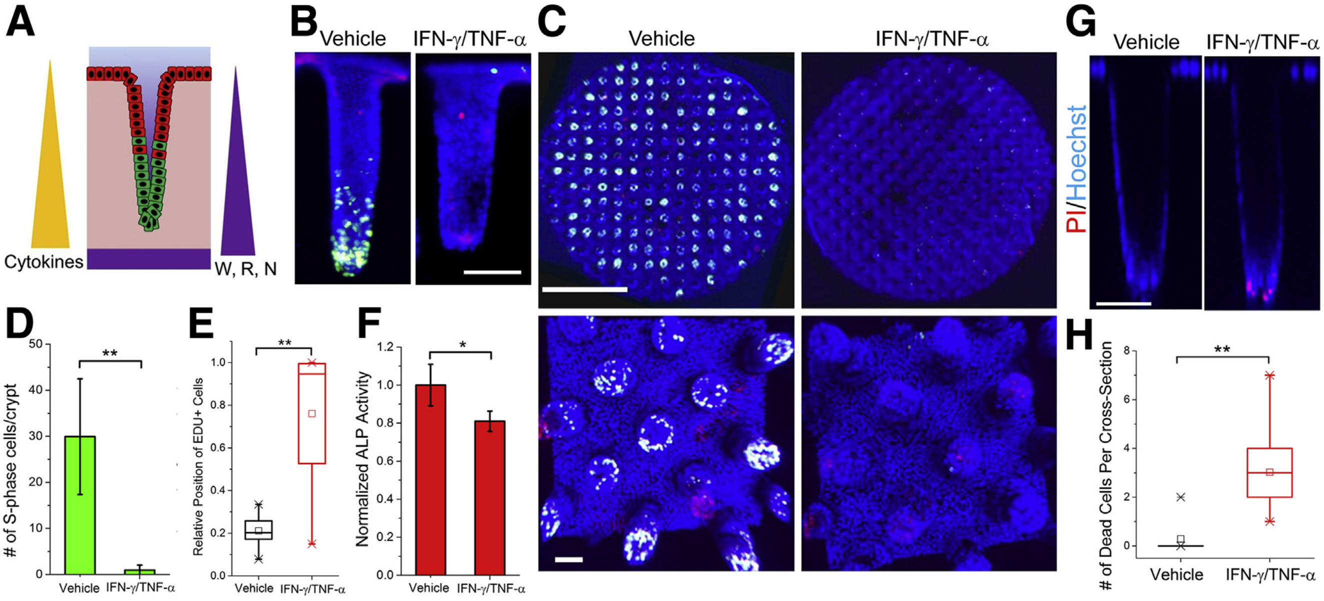

Figure 6. The effect of the cytokines, IFN-γ and TNF-α, on in vitro human crypts. (*A*) Biochemical gradients applied to the tissue. (*B*) Side view of representative crypts from the arrays under gradients of vehicle (0.1% BSA, control), or cytokines of 10 ng/mL IFN-γ and 100 ng/mL TNF-α. *Scale bar*: 100 μm. Red, ALP; green, EdU-based stain; blue, DNA. (*C*) Confocal 3-dimensional reconstruction of human crypt array viewed from basal side. *Upper panel scale bar*: 1 mm; *lower panel scale bar*: 100 μm. (*D*) Effect of cytokine gradient on number of EdU$^+$ cells per crypt (N = 20 crypts). (*E*) *Box plot* showing the relative position of EdU$^+$ cells along the basal–luminal axis of crypts. Zero represents the basal end of the crypt and 1 marks the luminal end of the crypt. (*F*) Normalized ALP stain for the array with the focal plane at the luminal side with a depth of field of 60 μm (N = 4 arrays). (*G*) A cross-sectional image through an in vitro crypt obtained by confocal fluorescence imaging. *Left*: Crypt in the absence of a cytokine gradient. *Right*: Crypt in the presence of an IFN-γ/TNF-α gradient. The cells were stained with Hoechst 33342 (blue) and propidium iodide (PI) (red). *Scale bar*: 100 μm. (*H*) *Box plot* depicting the number of dead cells per cross-section of crypt (N ≥ 24). Unpaired 2-tailed Student *t* test: $^*P < .05$; $^{**}P < .005$. N, noggin; R, R-spondin; W, Wnt-3A.

proliferation along the crypt axis consistent with their reported behavior in organoid systems (Figure 5*B*–*E*).[48] In contrast, the butyrate gradient eliminated cell proliferation in the luminal crypt region as shown by the absence of EdU$^+$ cells from the upper crypt half (Figure 5*B*–*E*). Cell proliferation also was diminished but not eliminated near the crypt base so that butyrate acted to restrict the proliferating cells to the very base of the crypt. Dose-response experiments showed that each butyrate concentration (0.5–5 mmol/L) diminished stem/progenitor cell turnover (Figure 5*G* and *H*), whereas only the higher concentrations (2–5 mmol/L) enhanced absorptive colonocyte formation. Previous SCFA studies have been reliant on colon cancer cell lines that do not accurately model the colonic epithelium.[51] Using our in vitro crypt platform, we show that butyrate suppresses stem cell activity, which supports the hypothesized effect of butyrate in human beings,[48] and is capable of inducing the differentiation of colonocytes into the absorptive lineage. This latter finding has broad-ranging implications because it is evidence linking microbial metabolites with cell-fate decisions in human beings.

Perturbation of In Vitro Crypts by Cytokines

Inflammatory cytokines such as IFN-γ and TNF-α are produced in significant quantities by the inflamed intestine.[52] For example, IFN-γ and TNF-α were found to be the most highly induced cytokines in dextran sulfate–treated colon.[52] However, the exact effect of these cytokines has been quite challenging to identify because of the plethora of changes ongoing in animals with inflamed intestine. As a result, many studies have relied on tissue-cultured cell lines, such as the T84 colon carcinoma line, as surrogate reporter systems. In this cell system, TNF-α and IFN-γ synergistically suppress proliferation.[52] Further complicating the understanding of cytokine impact is that these molecules likely exist at different concentrations within the crypt, which may modulate their impact on the various cell types.[52–54] To

Figure 5. (***See previous page***). **Modulation of in vitro human crypts by SCFAs.** (*A*) Biochemical gradients applied to the tissue. (*B*) Side view of representative crypts from the arrays (*scale bar*: 100 μm) under different SCFA gradients: no SCFA gradient (control), acetate (0–15 mmol/L), propionate (0–5 mmol/L), and butyrate (0–5 mmol/L). Red, ALP; green, EdU-based stain; blue, DNA. (*C*) Top view of human crypt array. *Upper panel scale bar*: 1 mm; *lower panel scale bar*: 100 μm. (*D*) Number of EdU$^+$ cells per crypt under different gradients. (*E*) Relative proliferation length, defined as the length of EdU$^+$ crypt over the total length of the crypt for the different gradients. (*F*) Normalized ALP activity for the various SCFA gradients. (*G and H*) EdU incorporation and ALP activity under different butyrate gradients. Basal butyrate (0 mmol/L) with the luminal butyrate concentration listed on the x-axis. N, noggin; R, R-spondin; W, Wnt-3A. $^*P < .05$ and $^{**}P < .005$.

determine whether the in vitro colon crypts are responsive to inflammatory cytokines, the tissue was cultured under a gradient of growth factors and cytokines (100 ng/mL TNF-α and 10 ng/mL IFN-γ) applied from the basal side for 4 days (Figure 5*A*). The cytokines were included in the basal compartment because they are produced by various cells of the mucosal immune system in response to environmental triggers.[53] Cell proliferation as measured by EdU incorporation under a gradient of cytokines was dramatically suppressed in the crypts when compared with the vehicle control (0.1% BSA) (Figure 5*B*–*E*). The cytokines eliminated tissue polarity because most crypts exposed to the cytokines possessed no EdU$^+$ cells at any location within the crypt. In the small number of crypts that did possess EdU$^+$ cells, the cells were located randomly (Figure 5*B* and *E*). The number of S-phase (EdU$^+$) cells per crypt decreased from 30 ± 13 for the control tissue to 1 ± 1 in that exposed to cytokine (Figure 5*D*). In contrast, the cytokines only slightly decreased the ALP activity relative to that of control (Figure 5*F*). To determine whether the decrease in proliferation under the cytokine gradient was a result of cell death, the crypt arrays were stained with Hoechst 33342 and propidium iodide. The cytokine-exposed tissue possessed significantly more dead cells (propidium iodide positive) than that without cytokine (Figure 6*A*–*H*); however, the absolute numbers of dead cells per crypt was low in both instances. Thus, the loss in cell proliferation was not owing to the death of the cells within tissue but rather owing to diminished numbers of viable cells in the S phase. These data show that the basally released inflammatory cytokines diminish the self-renewal power of the crypts.

Conclusions

Stem cells obtained from a human colon biopsy specimen were used to create self-renewing mimics of colonic crypts. Chemical gradients applied across the tissue construct led to compartmentalization of the stem/progenitor cells and promoted appropriate lineage differentiation and cell movement replicating human crypt biology. Application of gradients of microbiota-derived fermentation products drove alterations in the size of the crypts' proliferative and differentiated compartments as predicted to occur in vivo. Construction of primary epithelium from human stem cells yields a physiologically relevant mimic of the colonic epithelium, bringing to fruition an in vitro human tissue platform for the study of drugs and microbiome-derived compounds.

References

1. Picollet-D'hahan N, Dolega ME, Liguori L, Marquette C, Le Gac S, Gidrol X, Martin DK. A 3D toolbox to enhance physiological relevance of human tissue models. Trends Biotechnol 2016;34:757–769.
2. Bhise NS, Ribas J, Manoharan V, Zhang YS, Polini A, Massa S, Dokmeci MR, Khademhosseini A. Organ-on-a-chip platforms for studying drug delivery systems. J Control Release 2014;190:82–93.
3. van der Meer AD, van den Berg A. Organs-on-chips: breaking the in vitro impasse. Integr Biol (Camb) 2012;4:461–470.
4. Polini A, Prodanov L, Bhise NS, Manoharan V, Dokmeci MR, Khademhosseini A. Organs-on-a-chip: a new tool for drug discovery. Expert Opin Drug Discov 2014;9:335–352.
5. Power SE, O'Toole PW, Stanton C, Ross RP, Fitzgerald GF. Intestinal microbiota, diet and health. Br J Nutr 2014;111:387–402.
6. Gareau MG, Sherman PM, Walker WA. Probiotics and the gut microbiota in intestinal health and disease. Nat Rev Gastroenterol Hepatol 2010;7:503–514.
7. Kim H-J, Ingber DE. Gut-on-a-chip microenvironment induces human intestinal cells to undergo villus differentiation. Integr Biol (Camb) 2013;5:1130–1140.
8. Kim HJ, Huh D, Hamilton G, Ingber DE. Human gut-on-a-chip inhabited by microbial flora that experiences intestinal peristalsis-like motions and flow. Lab Chip 2012;12:2165–2174.
9. Chen Y, Lin YN, Davis KM, Wang QR, Rnjak-Kovacina J, Li CM, Isberg RR, Kumamoto CA, Mecsas J, Kaplan DL. Robust bioengineered 3D functional human intestinal epithelium. Sci Rep 2015;5:13708.
10. Sung JH, Yu J, Luo D, Shuler ML, March JC. Microscale 3-D hydrogel scaffold for biomimetic gastrointestinal (GI) tract model. Lab Chip 2011;11:389–392.
11. van der Flier LG, Clevers H. Stem cells, self-renewal, and differentiation in the intestinal epithelium. Ann Rev Physiol 2009;71:241–260.
12. Ranga A, Gjorevski N, Lutolf MP. Drug discovery through stem cell-based organoid models. Adv Drug Deliv Rev 2014;69:19–28.
13. Sato T, Stange DE, Ferrante M, Vries RG, Van Es JH, Van den Brink S, Van Houdt WJ, Pronk A, Van Gorp J, Siersema PD, Clevers H. Long-term expansion of epithelial organoids from human colon, adenoma, adenocarcinoma, and Barrett's epithelium. Gastroenterology 2011;141:1762–1772.
14. Miyoshi H, Stappenbeck TS. In vitro expansion and genetic modification of gastrointestinal stem cells in spheroid culture. Nat Protoc 2013;8:2471–2482.
15. Yui SR, Nakamura T, Sato T, Nemoto Y, Mizutani T, Zheng X, Ichinose S, Nagaishi T, Okamoto R, Tsuchiya K, Clevers H, Watanabe M. Functional engraftment of colon epithelium expanded in vitro from a single adult Lgr5(+) stem cell. Nat Med 2012;18:618–623.
16. Bermudez-Brito M, Plaza-Diaz J, Fontana L, Munoz-Quezada S, Gil A. In vitro cell and tissue models for studying host-microbe interactions: a review. Br J Nutr 2013;109(Suppl 2):S27–S34.
17. Brugmann SA, Wells JM. Building additional complexity to in vitro-derived intestinal tissues. Stem Cell Res Ther 2013;4(Suppl 1):S1.
18. Foulke-Abel J, In J, Kovbasnjuk O, Zachos NC, Ettayebi K, Blutt SE, Hyser JM, Zeng XL, Crawford SE, Broughman JR, Estes MK, Donowitz M. Human enteroids as an ex-vivo model of host-pathogen interactions in the gastrointestinal tract. Exp Biol Med 2014;239:1124–1134.

19. Kuratnik A, Giardina C. Intestinal organoids as tissue surrogates for toxicological and pharmacological studies. Biochem Pharmacol 2013;85:1721–1726.
20. Sato T, Clevers H. Growing self-organizing mini-guts from a single intestinal stem cell: mechanism and applications. Science 2013;340:1190–1194.
21. Gjorevski N, Sachs N, Manfrin A, Giger S, Bragina ME, Ordóñez-Morán P, Clevers H, Lutolf MP. Designer matrices for intestinal stem cell and organoid culture. Nature 2016;539:560–564.
22. Sato T, Vries RG, Snippert HJ, van de Wetering M, Barker N, Stange DE, van Es JH, Abo A, Kujala P, Peters PJ, Clevers H. Single Lgr5 stem cells build crypt-villus structures in vitro without a mesenchymal niche. Nature 2009;459:262–U147.
23. Huch M, Knoblich JA, Lutolf MP, Martinez-Arias A. The hope and the hype of organoid research. Development 2017;144:938–941.
24. Kerstin S, Bart S, Pedro C, Norman S, Hans C, Jos M. Converging biofabrication and organoid technologies: the next frontier in hepatic and intestinal tissue engineering? Biofabrication 2017;9:013001.
25. Wang Y, DiSalvo M, Gunasekara DB, Dutton J, Proctor A, Lebhar MS, Williamson IA, Speer J, Howard RL, Smiddy NM, Bultman SJ, Sims CE, Magness ST, Allbritton NL. Self-renewing monolayer of primary colonic or rectal epithelial cells. Cell Mol Gastroenterol Hepatol 2017;4:165–182.e7.
26. Wang Y, Gunasekara DB, Reed MI, DiSalvo M, Bultman SJ, Sims CE, Magness ST, Allbritton NL. A microengineered collagen scaffold for generating a polarized crypt-villus architecture of human small intestinal epithelium. Biomaterials 2017;128:44–55.
27. Wang Y, Ahmad AA, Shah PK, Sims CE, Magness ST, Allbritton NL. Capture and 3D culture of colonic crypts and colonoids in a microarray platform. Lab Chip 2013;13:4625–4634.
28. Wang Y, Ahmad AA, Sims CE, Magness ST, Allbritton NL. In vitro generation of colonic epithelium from primary cells guided by microstructures. Lab Chip 2014;14:1622–1631.
29. Ahmad AA, Wang YL, Gracz AD, Sims CE, Magness ST, Allbritton NL. Optimization of 3-D organotypic primary colonic cultures for organ-on-chip applications. J Biol Eng 2014;8:9.
30. Wang Y, Dhopeshwarkar R, Najdi R, Waterman ML, Sims CE, Allbritton N. Microdevice to capture colon crypts for in vitro studies. Lab Chip 2010;10:1596–1603.
31. Ahmad AA, Wang YL, Sims CE, Magness ST, Allbritton NL. Optimizing Wnt-3a and R-spondin1 concentrations for stem cell renewal and differentiation in intestinal organoids using a gradient-forming microdevice. RSC Adv 2015;5:74881–74891.
32. Attayek PJ, Ahmad AA, Wang Y, Williamson I, Sims CE, Magness ST, Allbritton NL. In vitro polarization of colonoids to create an intestinal stem cell compartment. PLoS One 2016;11:e0153795.
33. van de Wetering M, Francies HE, Francis JM, Bounova G, Iorio F, Pronk A, van Houdt W, van Gorp J, Taylor-Weiner A, Kester L, McLaren-Douglas A, Blokker J, Jaksani S, Bartfeld S, Volckman R, van Sluis P, Li VSW, Seepo S, Pedamallu CS, Cibulskis K, Carter SL, McKenna A, Lawrence MS, Lichtenstein L, Stewart C, Koster J, Versteeg R, van Oudenaarden A, Saez-Rodriguez J, Vries RGJ, Getz G, Wessels L, Stratton MR, McDermott U, Meyerson M, Garnett MJ, Clevers H. Prospective derivation of a living organoid biobank of colorectal cancer patients. Cell 2015;161:933–945.
34. Yin XL, Farin HF, van Es JH, Clevers H, Langer R, Karp JM. Niche-independent high-purity cultures of Lgr5(+) intestinal stem cells and their progeny. Nat Methods 2014;11:106–112.
35. Pai JH, Wang Y, Salazar GT, Sims CE, Bachman M, Li GP, Allbritton NL. Photoresist with low fluorescence for bioanalytical applications. Anal Chem 2007;79:8774–8780.
36. Hu SW, Ren XQ, Bachman M, Sims CE, Li GP, Allbritton N. Surface modification of poly(dimethylsiloxane) microfluidic devices by ultraviolet polymer grafting. Anal Chem 2002;74:4117–4123.
37. Woo HJ, Yoo WJ, Bae CH, Song SY, Kim YW, Park SY, Kim YD. Leptin up-regulates MUC5B expression in human airway epithelial cells via mitogen-activated protein kinase pathway. Exp Lung Res 2010;36:262–269.
38. Van der Flier LG, Haegebarth A, Stange DE, Van de Wetering M, Clevers H. OLFM4 is a robust marker for stem cells in human intestine and marks a subset of colorectal cancer cells. Gastroenterology 2009;137:15–17.
39. Jung P, Sato T, Merlos-Suarez A, Barriga FM, Iglesias M, Rossell D, Auer H, Gallardo M, Blasco MA, Sancho E, Clevers H, Batlle E. Isolation and in vitro expansion of human colonic stem cells. Nat Med 2011;17:1225–1227.
40. Kosinski C, Li VSW, Chan ASY, Zhang J, Ho C, Tsui WY, Chan TL, Mifflin RC, Powell DW, Yuen ST, Leung SY, Chen X. Gene expression patterns of human colon tops and basal crypts and BMP antagonists as intestinal stem cell niche factors. Proc Natl Acad Sci U S A 2007;104:15418–15423.
41. Barker N. Adult intestinal stem cells: critical drivers of epithelial homeostasis and regeneration. Nat Rev Mol Cell Biol 2014;15:19–33.
42. Watson AJM, Duckworth CA, Guan YF, Montrose MH. Mechanisms of epithelial cell shedding in the mammalian intestine and maintenance of barrier function. In: Fromm M, Schulzke JD, eds. Molecular structure and function of the tight junction: from basic mechanisms to clinical manifestations, 1165; 2009:135–142.
43. Cayo MA, Cayo AK, Jarjour SM, Chen H. Sodium butyrate activates Notch1 signaling, reduces tumor markers, and induces cell cycle arrest and apoptosis in pheochromocytoma. Am J Transl Res 2009;1:178–183.
44. Geling A, Steiner H, Willem M, Bally-Cuif L, Haass C. A gamma-secretase inhibitor blocks Notch signaling in vivo and causes a severe neurogenic phenotype in zebrafish. EMBO Rep 2002;3:688–694.
45. Yang CR. Enhanced physicochemical properties of collagen by using EDC/NHS-crosslinking. Bull Mater Sci 2012;35:913–918.

46. Moutairou K, Fritsch P, Meslin JC, Poncy JL, Metivier H, Masse R. Epithelial cell migration on small intestinal villi in the neonatal rat. Comparison between [3H] thymidine and cytoplasmic labelling after Pu-citrate ingestion. Biol Cell 1989;65:265–269.
47. Cummings JH. Short chain fatty acids in the human colon. Gut 1981;22:763–779.
48. Kaiko GE, Ryu SH, Koues OI, Collins PL, Solnica-Krezel L, Pearce EJ, Pearce EL, Oltz EM, Stappenbeck TS. The colonic crypt protects stem cells from microbiota-derived metabolites. Cell 2016; 165:1708–1720.
49. Donohoe DR, Collins LB, Wali A, Bigler R, Sun W, Bultman SJ. The Warburg effect dictates the mechanism of butyrate-mediated histone acetylation and cell proliferation. Mol Cell 2012;48:612–626.
50. Wong JMW, de Souza R, Kendall CWC, Emam A, Jenkins DJA. Colonic health: fermentation and short chain fatty acids. J Clin Gastroenterol 2006;40:235–243.
51. Mariadason JM, Velcich A, Wilson AJ, Augenlicht LH, Gibson PR. Resistance to butyrate-induced cell differentiation and apoptosis during spontaneous Caco-2 cell differentiation. Gastroenterology 2001;120:889–899.
52. Nava P, Koch S, Laukoetter MG, Lee WY, Kolegraff K, Capaldo CT, Beeman N, Addis C, Gerner-Smidt K, Neumaier I, Skerra A, Li LH, Parkos CA, Nusrat A. Interferon-gamma regulates intestinal epithelial homeostasis through converging beta-catenin signaling pathways. Immunity 2010;32:392–402.
53. Neurath MF. Cytokines in inflammatory bowel disease. Nat Rev Immunol 2014;14:329–342.
54. Osaki LH, Mills JC. A perfect match: explant and organoid systems help study cytokines in sickness and health. Cell Mol Gastroenterol Hepatol 2017;3:4–5.

Received July 29, 2017. Accepted October 26, 2017.

Correspondence
Address correspondence to: Nancy L. Allbritton, MD, PhD, Department of Biomedical Engineering, Chapman Hall, Room 241, University of North Carolina, Chapel Hill, North Carolina. e-mail: nlallbri@unc.edu or nlallbri@ncsu.edu; fax: (919) 962-5203.

Acknowledgments
The authors thank Bailey Altizer for coordinating the procurement of human colonic biopsy specimens.

Author contributions
Yuli Wang, Scott J. Bultman, Christopher E. Sims, Scott T. Magness, and Nancy L. Allbritton designed experiments; Yuli Wang and Raehyun Kim performed experiments; Dulan B. Gunasekara, Matthew DiSalvo, Mark I. Reed, and Daniel L. Nguyen provided technical support; Yuli Wang, Raehyun Kim, Matthew DiSalvo, and Nancy L. Allbritton analyzed data; Yuli Wang and Nancy L. Allbritton administered experiments; and Yuli Wang, Scott J. Bultman, Christopher E. Sims, Scott T. Magness, and Nancy L. Allbritton wrote the paper.

Conflicts of interest
These authors disclose the following: Yuli Wang, Christopher E. Sims, Scott T. Magness, and Nancy L. Allbritton have a financial interest in Altis Biosystems. The remaining authors disclose no conflicts.

Funding
Supported by the National Institutes of Health, National Institute of Diabetes and Digestive and Kidney Diseases award R01DK109559 (N.L.A., S.J.B., and S.T.M.).